Catal Lett (2008) 124:364–368
DOI 10.1007/s10562-008-9476-7

Effect of Divalent Metal Component (Me^{II}) on the Catalytic Performance of $Me^{II}Fe_2O_4$ Catalysts in the Oxidative Dehydrogenation of n-Butene to 1,3-Butadiene

Howon Lee · Ji Chul Jung · Heesoo Kim · Young-Min Chung · Tae Jin Kim · Seong Jun Lee · Seung-Hoon Oh · Yong Seung Kim · In Kyu Song

Received: 9 March 2008 / Accepted: 12 March 2008 / Published online: 12 April 2008

Abstract A series of metal ferrite ($Me^{II}Fe_2O_4$) catalysts were prepared by a co-precipitation method with a variation of divalent metal component (Me^{II} = Zn, Mg, Mn, Ni, Co, and Cu) for use in the oxidative dehydrogenation of n-butene to 1,3-butadiene. Successful formation of metal ferrite catalysts with a random spinel structure was confirmed by XRD, ICP-AES, and XPS analyses. The catalytic performance of metal ferrite catalysts in the oxidative dehydrogenation of n-butene strongly depended on the identity of divalent metal component. Acid properties of metal ferrite catalysts were measured by NH_3-TPD experiments, with an aim of correlating the catalytic performance with the acid property of the catalysts. It was revealed that the yield for 1,3-butadiene increased with increasing surface acidity of the catalyst. Among the catalysts tested, $ZnFe_2O_4$ catalyst with the largest surface acidity showed the best catalytic performance in the oxidative dehydrogenation of n-butene.

Keywords n-Butene · 1,3-Butadiene · Oxidative dehydrogenation · Ferrite catalyst · Surface acidity

1 Introduction

Selective oxidation of olefins has been considered to be an important subject for the production of various chemical intermediates in the petrochemical industries [1–4]. In particular, oxidative dehydrogenation of n-butene has attracted much attention as a promising process for producing 1,3-butadiene, an important raw material for manufacturing a large number of chemicals such as ABS (acrylonitrile-butadiene-styrene), BR (butadiene rubber), and SBR (styrene-butadiene rubber) [4–6]. A number of catalysts have been investigated for the oxidative dehydrogenation of n-butene, including ferrite-type catalyst [7–10], Cu-Mo catalyst [11], vanadium-containing catalyst [12], and Bi-Mo-based catalyst [13, 14]. Among these catalysts, metal ferrite catalysts have been extensively studied as efficient catalysts for this reaction [15–17].

Metal ferrite catalysts have a general form of $Me^{II}Fe_2O_4$ such as $ZnFe_2O_4$ (zinc ferrite), $MgFe_2O_4$ (magnesium ferrite), $CoFe_2O_4$ (cobalt ferrite), and $CuFe_2O_4$ (copper ferrite) [15–17]. It can be inferred that the identity of divalent metal component (Me^{II}) inevitably affects the catalytic performance of metal ferrite catalysts in the oxidative dehydrogenation of n-butene. Nonetheless, no systematic investigations on the effect of divalent metal component on the catalytic performance of metal ferrite catalysts in the oxidative dehydrogenation of n-butene have been reported yet.

Many attempts have been made to find a crucial factor determining the catalytic performance in the oxidative dehydrogenation of n-butene [18, 19]. Although the fundamental reaction mechanism has not been clearly elucidated, many researchers agree that the reaction mechanism by way of π-allyl intermediate is the most feasible reaction pathway for the formation of 1,3-butadiene from n-butene [6, 18, 20, 21]. According to this mechanism, an initial abstraction of α-hydrogen from n-butene to form π-allyl intermediate is the rate-determining step in the oxidative dehydrogenation of n-butene. This means that acid property of the catalyst plays a very important role in abstracting α-hydrogen from

H. Lee · J. C. Jung · H. Kim · I. K. Song (✉)
School of Chemical and Biological Engineering, Institute of Chemical Processes, Seoul National University, Shinlim-dong, Kwanak-ku, Seoul 151-744, South Korea
e-mail: inksong@snu.ac.kr

Y.-M. Chung · T. J. Kim · S. J. Lee · S.-H. Oh · Y. S. Kim
SK Energy Corporation, Yuseong-ku, Daejeon 305-712, South Korea

n-butene (a base molecule) in this reaction [22, 23]. It has been demonstrated in our previous works [15, 24] that the catalytic performance of zinc ferrite catalyst in the oxidative dehydrogenation of n-butene was closely related to the surface acidity of the catalyst.

In this work, a series of metal ferrite ($Me^{II}Fe_2O_4$) catalysts with different divalent metal (Me^{II} = Zn, Mg, Mn, Ni, Co, and Cu) were prepared by a co-precipitation method, and were applied to the oxidative dehydrogenation of n-butene to 1,3-butadiene. The formation of metal ferrite catalysts was confirmed by XRD, ICP-AES, and XPS analyses. NH_3-TPD experiments were conducted to measure the acid properties of metal ferrite catalysts. A correlation between catalytic performance and acid property of metal ferrite catalysts was then established.

2 Experimental

2.1 Preparation of Metal Ferrite ($Me^{II}Fe_2O_4$) catalysts

Metal ferrite ($Me^{II}Fe_2O_4$) catalysts with different divalent metal (Me^{II} = Zn, Mg, Mn, Ni, Co, and Cu) were prepared by a co-precipitation method. A total of 1,000 mL of sodium hydroxide solution (0.6 N NaOH from Sigma-Aldrich) was heated to 70 °C. 1.42 g of zinc chloride ($ZnCl_2$ from Sigma-Aldrich) and 5.61 g of iron chloride ($FeCl_3 \cdot 6H_2O$ from Sigma-Aldrich) were separately dissolved in 100 mL of distilled water at 70 °C. The metal precursor solutions were then added into the sodium hydroxide solution as quickly as possible under vigorous stirring. After the resulting solution was stirred vigorously at 70 °C for 1 h, it was aged overnight at room temperature. The precipitate was filtered and washed with distilled water to obtain a solid product. The solid product was dried at 175 °C for 16 h, and finally, it was calcined at 475 °C for 3 h to yield the zinc ferrite ($ZnFe_2O_4$) catalyst. 1.19 g of magnesium chloride ($MgCl_2$ from Sigma-Aldrich), 2.15 g of manganese chloride ($MnCl_2 \cdot 4H_2O$ from Sigma-Aldrich), 2.54 g of nickel chloride ($NiCl_2 \cdot 6H_2O$ from Sigma-Aldrich), 2.54 g of cobalt chloride ($CoCl_2 \cdot 6H_2O$ from Sigma-Aldrich), and 1.78 g of copper chloride ($CuCl_2 \cdot 2H_2O$ from Sigma-Aldrich) were used as a divalent metal precursor for the preparation of corresponding metal ferrite catalyst.

2.2 Characterization

Formation of metal ferrite ($Me^{II}Fe_2O_4$) catalysts was confirmed by XRD (MAC Science, M18XHF-SRA) measurements. Atomic ratios of constituent metal components in the prepared catalysts were determined by ICP-AES (Shimadz, ICP-1000IV) analyses. Surface areas of the catalysts were measured using a BET apparatus (Micromeritics, ASAP 2010). XPS analyses (Thermo VG, Sigma Probe) were conducted to measure the binding energies of Fe ions in the metal ferrite catalysts using C 1s peak (284.6 eV) as a reference.

Acid properties of metal ferrite catalysts were measured by NH_3-TPD experiments. Each catalyst (0.3 g) was charged into a tubular quartz reactor of the conventional TPD apparatus. The catalyst was pretreated at 200 °C for 1 h under a flow of helium (20 mL/min) to remove any physisorbed organic molecules. About 20 mL of NH_3 was then pulsed into the reactor every minute at room temperature under a flow of helium (5 mL/min), until the acid sites were saturated with NH_3. The physisorbed NH_3 was removed by evacuating the catalyst sample at 50 °C for 1 h. The furnace temperature was increased from room temperature to 600 °C at a heating rate of 5 °C/min under a flow of helium (10 mL/min). The desorbed NH_3 was detected using a GC-MSD (Agilent, MSD-6890N GC).

2.3 Oxidative Dehydrogenation of n-Butene

Oxidative dehydrogenation of n-butene to 1,3-butadiene was carried out in a continuous flow fixed-bed reactor in the presence of air and steam. Each catalyst (0.33 g) was pretreated at 470 °C for 1 h with an air stream (16 mL/min). Water was sufficiently vaporized by passing through a pre-heating zone and continuously fed into the reactor together with n-butene and air. C_4 raffinate-3 containing 57.9 wt.% n-butene (1-butene (7.5 wt.%) + trans-2-butene (33.9 wt.%) + cis-2-butene (16.5 wt.%)) was used as a n-butene source, and air was used as an oxygen source (nitrogen in air served as a carrier gas). Feed composition was fixed at n-butene:oxygen:steam = 1:0.75:15. The catalytic reaction was carried out at 420 °C. GHSV (gas hourly space velocity) was fixed at 475 h^{-1} on the basis of n-butene. Reaction products were periodically sampled and analyzed with gas chromatographs. Conversion of n-butene and selectivity for 1,3-butadiene were calculated on the basis of carbon balance as follows. Yield for 1,3-butadiene was calculated by multiplying conversion and selectivity.

$$\text{Conversion of n-butene} = \frac{\text{moles of n-butene reacted}}{\text{moles of n-butene supplied}}$$

$$\text{Selectivity for 1,3-butadiene} = \frac{\text{moles of 1,3-butadiene formed}}{\text{moles of n-butene reacted}}$$

3 Results and Discussion

3.1 Formation of Metal Ferrite ($Me^{II}Fe_2O_4$) Catalysts

Successful formation of metal ferrite ($Me^{II}Fe_2O_4$) catalysts was confirmed by XRD and ICP-AES measurements.

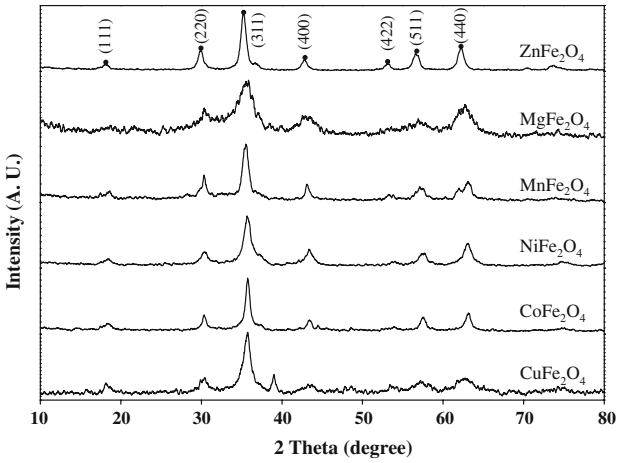

Fig. 1 XRD patterns of $Me^{II}Fe_2O_4$ (Me^{II} = Zn, Mg, Mn, Ni, Co, and Cu) catalysts

Figure 1 shows the XRD patterns of metal ferrite catalysts with different divalent metal (Me^{II} = Zn, Mg, Mn, Ni, Co, and Cu). Each phase was identified by its characteristic diffraction peaks using JCPDS. The XRD patterns are in good agreement with those reported in previous works [16, 19, 25], indicating the successful formation of metal ferrite catalysts. As listed in Table 1, Fe/Me^{II} atomic ratios of metal ferrite catalysts determined by ICP-AES analyses were in the range of 1.90–2.15, in good agreement with the theoretical value of 2.0. This result also supports that metal ferrite catalysts were successfully prepared in this work. BET surface areas of metal ferrite catalysts are also summarized in Table 1.

To confirm the structure of metal ferrite catalysts, binding energies of Fe cations were measured by XPS analyses. Metal ferrite catalysts have a spinel crystalline structure (AB_2O_4) with tetrahedral and octahedral sites for metal atoms [26]. Three types of spinel structures (normal spinel, inverse spinel, and random spinel) can be formed depending on the distribution of metal atoms; (i) a normal spinel structure in which divalent cations (A) are in the tetrahedral sites and trivalent cations (B) are in the octahedral sites, (ii) an inverse spinel structure in which divalent cations (A) occupy octahedral sites while trivalent cations (B) are equally distributed in the tetrahedral and octahedral sites, and (iii) a random spinel structure in which divalent (A) and trivalent cations (B) are randomly located at both tetrahedral and octahedral sites [7, 27]. In the metal ferrite catalysts with a form of $Me^{II}Fe_2O_4$, therefore, Fe cations can be located at two different sites (tetrahedral and octahedral sites) in the spinel crystalline structure [21, 27]. This means that the type of spinel structure of metal ferrite catalysts can be identified by determining the location of Fe cations in the spinel structure. To identify the spinel structure of metal ferrite catalysts, XPS analyses for measuring the binding energies of Fe cations of metal ferrite catalysts were conducted.

Table 1 Atomic ratios and BET surface areas of metal ferrite ($Me^{II}Fe_2O_4$) catalysts

Me^{II}	Atomic ratio of Fe/Me^{II}	BET surface area (m^2/g)
Zn	2.15	76.5
Mg	1.90	151.1
Mn	1.91	100.3
Ni	2.10	102.4
Co	2.00	105.3
Cu	2.02	90.1

Figure 2 shows the XPS spectrum of Fe^{3+} $2p_{3/2}$ of $ZnFe_2O_4$ catalyst. Deconvolution of the spectrum reveals that there are two types of Fe cations in the $ZnFe_2O_4$ catalyst which are located at the tetrahedral and octahedral sites. These two types of Fe cations were also observed in all the $Me^{II}Fe_2O_4$ catalysts. The binding energies of Fe^{3+} $2p_{3/2}$ of metal ferrite catalysts are summarized in Table 2.

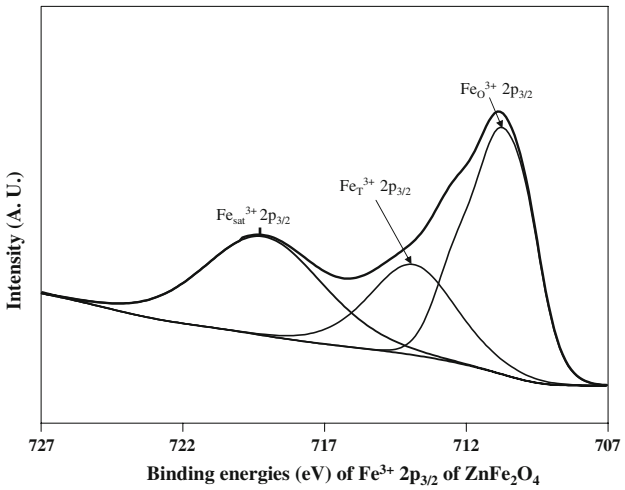

Fig. 2 XPS spectrum of Fe^{3+} $2p_{3/2}$ of $ZnFe_2O_4$ catalyst

Table 2 Binding energies of Fe^{3+} $2p_{3/2}$ of metal ferrite ($Me^{II}Fe_2O_4$) catalysts

Me^{II}	Binding energy (eV)			I^a (%)
	Fe_O^{3+} $2p_{3/2}$	Fe_T^{3+} $2p_{3/2}$	Fe_{Sat}^{3+} $2p_{3/2}$	
Zn	710.9	714.0	719.3	32.2
Mg	710.3	713.3	718.5	33.2
Mn	710.7	713.8	719.1	34.2
Ni	710.3	713.2	718.4	33.9
Co	710.8	714.1	718.9	35.9
Cu	710.3	713.2	718.3	37.6

[a] Amount of Fe^{3+} located at the tetrahedral site

$$I^a\ (\%) = \frac{\text{Area of } Fe_T^{3+}2p_{3/2} \text{ peak}}{\text{Area of } Fe_T^{3+}2p_{3/2} \text{ peak} + \text{Area of } Fe_O^{3+}2p_{3/2} \text{ peak}} \times 100$$

It is noticeable that all the $Me^{II}Fe_2O_4$ catalysts retained a satellite peak (Fe^{3+}_{sat} $2p_{3/2}$) within the range of 718.3–719.3 eV, indicating that all Fe cations of $Me^{II}Fe_2O_4$ catalysts are trivalent cations (Fe^{3+}) [28]. A peak within the range of 710.3–710.9 eV was attributed to the Fe^{3+} cations located at the octahedral site (Fe^{3+}_{O} $2p_{3/2}$) in the spinel crystalline structure, while a peak within the range of 713.2–714.1 eV was due to the Fe^{3+} cations located at the tetrahedral site (Fe^{3+}_{T} $2p_{3/2}$) in the spinel crystalline structure [25]. The amounts of Fe^{3+} cations located at the tetrahedral site of metal ferrite catalysts are also summarized in Table 2. The result clearly shows that ca. 1/3 (32.2–37.6 %) of Fe^{3+} cations is located at the tetrahedral site of metal ferrite catalysts, regardless of the different identity of divalent metal. This result indicates that all the metal ferrite catalysts prepared in this work have a random spinel structure.

3.2 Catalytic Performance of Metal Ferrite ($Me^{II}Fe_2O_4$) Catalysts

Figure 3 shows the catalytic performance of $Me^{II}Fe_2O_4$ (Me^{II} = Zn, Mg, Mn, Ni, Co, and Cu) catalysts in the oxidative dehydrogenation of n-butene at 420 °C after a 6 h-reaction. The catalytic performance was strongly dependent on the identity of divalent metal component. Conversion of n-butene, selectivity for 1,3-butadiene, and yield for 1,3-butadiene decreased in the order of $ZnFe_2O_4 > MgFe_2O_4 > MnFe_2O_4 > NiFe_2O_4 > CoFe_2O_4 > CuFe_2O_4$. Among the catalysts tested, $ZnFe_2O_4$ catalyst showed the highest yield for 1,3-butadiene (67.8%).

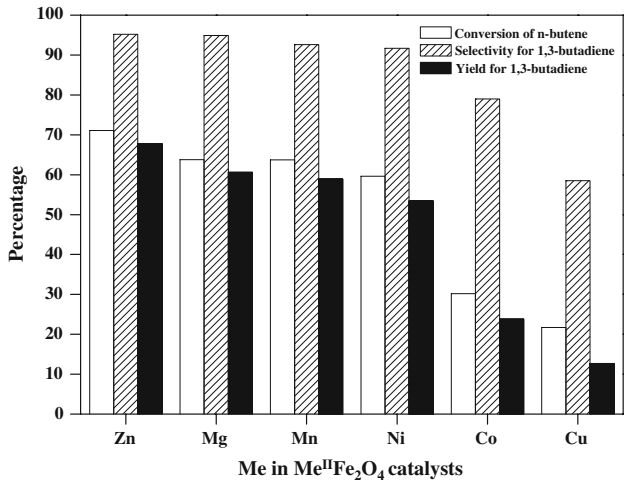

Fig. 3 Catalytic performance of $Me^{II}Fe_2O_4$ (Me^{II} = Zn, Mg, Mn, Ni, Co, and Cu) catalysts in the oxidative dehydrogenation of n-butene at 420 °C after a 6 h-reaction

3.3 Correlation Between Catalytic Performance and Surface Acidity

An attempt has been made to correlate the catalytic performance (Fig. 3) with the BET surface area (Table 1) of metal ferrite catalysts. However, the catalytic performance was not directly correlated with the BET surface area of metal ferrite catalysts. In order to investigate the effect of acid properties on the catalytic performance of metal ferrite catalysts, NH_3-TPD experiments were carried out. Figure 4 shows the NH_3-TPD profiles of selected metal ferrite catalysts. All the catalysts showed a broad NH_3-TPD peak. The metal ferrite catalysts exhibited a significant difference in total acidity (peak area) and a slight difference in acid strength (peak temperature) with a variation of divalent metal component (Me^{II}). We attempted to correlate the catalytic performance with the acid properties (acidity and acid strength) of metal ferrite catalysts. Unfortunately, either total acidity or acid strength was not directly correlated with the catalytic performance of metal ferrite catalysts. However, a reliable correlation between catalytic performance and surface acidity of the catalysts was observed. The surface acidity was defined as the amount of adsorbed NH_3 per unit surface area of a catalyst.

Figure 5 shows a correlation between yield for 1,3-butadiene and surface acidity of metal ferrite catalysts. The correlation clearly shows that the yield for 1,3-butadiene was closely related to the surface acidity of metal ferrite catalysts. This result was in good agreement with the previous work investigating the effect of acid property on the catalytic performance of zinc ferrite catalysts in the oxidative dehydrogenation of n-butene [15]. Among the catalysts tested, $ZnFe_2O_4$ catalyst with the largest surface acidity showed the best catalytic performance. As mentioned earlier, the acid property of metal ferrite catalysts plays an important role in adsorbing and activating n-butene, that is, in abstracting α-hydrogen from n-butene to form π-allyl intermediate

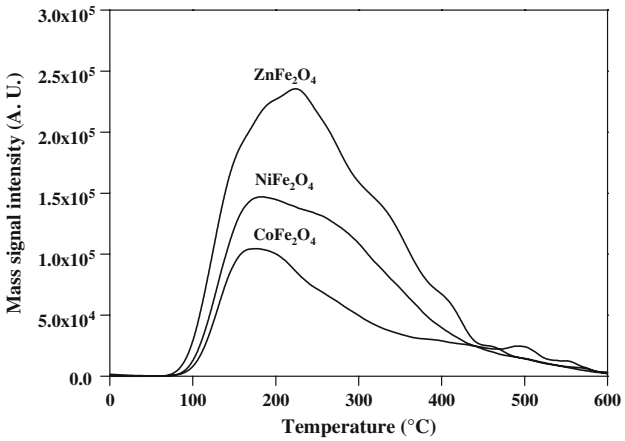

Fig. 4 NH_3-TPD profiles of selected metal ferrite catalysts

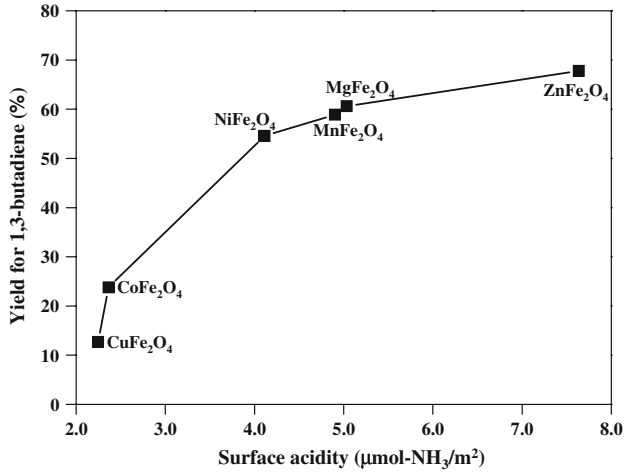

Fig. 5 A correlation between yield for 1,3-butadiene and surface acidity of metal ferrite catalysts

[15, 24]. Therefore, it is reasonable to expect that a catalyst with large surface acidity (with large capacity to activate n-butene per unit surface area) is favorable for the facile adsorption and activation of n-butene (a base molecule) in the oxidative dehydrogenation of n-butene. In conclusion, the surface acidity of metal ferrite catalysts played a key role in determining the catalytic performance in the oxidative dehydrogenation of n-butene.

4 Conclusions

Metal ferrite ($Me^{II}Fe_2O_4$) catalysts with different divalent metal (Me^{II} = Zn, Mg, Mn, Ni, Co, and Cu) were prepared by a co-precipitation method, and were applied to the oxidative dehydrogenation of n-butene to 1,3-butadiene. Successful formation of metal ferrite catalysts was well confirmed by XRD and ICP-AES analyses. XPS analyses for measuring the binding energies of Fe cations of metal ferrite catalysts revealed that all the metal ferrite catalysts retained a random spinel structure. Among the catalysts tested, $ZnFe_2O_4$ catalyst showed the best catalytic performance in the oxidative dehydrogenation of n-butene. The catalytic performance of metal ferrite catalyst was closely related to the surface acidity of the catalyst. The yield for 1,3-butadiene increased with increasing surface acidity of the catalyst. The largest surface acidity of $ZnFe_2O_4$ catalyst was responsible for its high catalytic performance in the oxidative dehydrogenation of n-butene.

Acknowledgments This work was supported by SK Energy Corporation (POST-BK21 Program) and Korea Energy Management Corporation (2005-01-0090-3-010).

References

1. Oh SC, Lee HP, Kim HT, Yoo KO (1999) Korean J Chem Eng 16:543–547
2. Kim YH, Yang HS (2000) Korean J Chem Eng 17:357–364
3. Kung HH (1986) Ind Eng Chem Prod Res Dev 25:171–178
4. Hong F, Yang BL, Schwartz LH, Kung HH (1984) J Phys Chem 88:2525–2530
5. Liaw BJ, Cheng DS, Yang BL (1989) J Catal 118:312–326
6. Toledo JA, Valenzuela MA, Armendáriz H, Aguilar-Ríos G, Zapata B, Montaya A, Nava N, Salas P, Schifter I (1995) Catal Lett 30:279–288
7. Rennard RJ, Kehl WL (1971) J Catal 21:282–293
8. Massoth FE, Scarpiello DA (1971) J Catal 21:294–302
9. Rennard RJ, Innes RA, Swift HE (1973) J Catal 30:128–138
10. Toledo-Antonio JA, Bosch P, Valenzuela MA, Montoya A, Nava N (1997) J Mol Catal A Chem 125:53–62
11. Tiwari PN, Alkhazov TG, Adzamov KU, Khanmamedova AK (1989) J Catal 120:278–281
12. López Nieto JM, Concepción P, Dejoz A, Knözinger H, Melo F, Vázquez MI (2000) J Catal 189:147–157
13. Jung JC, Lee H, Kim H, Chung YM, Kim TJ, Lee SJ, Oh SH, Kim YS, Song IK (2007) J Mol Catal A Chem 271:261–265
14. Jung JC, Lee H, Kim H, Chung YM, Kim TJ, Lee SJ, Oh SH, Kim YS, Song IK (2008) Catal Commun 9:447–452
15. Lee H, Jung JC, Kim H, Chung YM, Kim TJ, Lee SJ, Oh SH, Kim YS, Song IK (2008) Catal Commun 9:1137–1142
16. Gibson MA, Hightower JW (1976) J Catal 41:431–439
17. Cares WR, Hightower JW (1971) J Catal 23:193–203
18. Kung HH, Kung MC (1985) Adv Catal 33:159–198
19. Toledo-Antonio JA, Nava N, Martínez M, Bokhimi X (2002) Appl Catal A Gen 234:137–144
20. Gibson MA, Hightower JW (1976) J Catal 41:420–430
21. Xu WQ, Yin YG, Li GY, Chen S (1992) Appl Catal A Gen 89:131–142
22. Cullis CF, Hucknall DJ (1982) In: Bond GC, Webb G (eds) A specialist periodical report: catalysis, vol 5. Royal Chemical Society, London
23. Grasselli RK, Burrington JD (1981) Adv Catal 30:133–141
24. Lee H, Jung JC, Kim H, Chung YM, Kim TJ, Lee SJ, Oh SH, Kim YS, Song IK (2007) Catal Lett doi:10.1007/s10562-007-9371-7
25. Li F, Liu X, Yang Q, Liu J, Evans DG, Duan X (2005) Mater Res Bull 40:1244–1255
26. Jebarathinam NJ, Eswaramoorthy M, Krishnasamy V (1996) Appl Catal A Gen 145:57–74
27. Bid S, Pradhan SK (2003) Mater Chem Phys 82:27–37
28. Mullet M, Guillemin Y, Ruby C (2008) J Solid State Chem 181:81–89